



---

Extraterrestrial Cause for the Cretaceous-Tertiary Extinction

Author(s): Luis W. Alvarez, Walter Alvarez, Frank Asaro and Helen V. Michel

Source: *Science*, New Series, Vol. 208, No. 4448 (Jun. 6, 1980), pp. 1095-1108

Published by: [American Association for the Advancement of Science](#)

Stable URL: <http://www.jstor.org/stable/1683699>

Accessed: 19/09/2013 15:50

---

Your use of the JSTOR archive indicates your acceptance of the Terms & Conditions of Use, available at  
<http://www.jstor.org/page/info/about/policies/terms.jsp>

JSTOR is a not-for-profit service that helps scholars, researchers, and students discover, use, and build upon a wide range of content in a trusted digital archive. We use information technology and tools to increase productivity and facilitate new forms of scholarship. For more information about JSTOR, please contact support@jstor.org.



*American Association for the Advancement of Science* is collaborating with JSTOR to digitize, preserve and extend access to *Science*.

<http://www.jstor.org>

## Extraterrestrial Cause for the Cretaceous-Tertiary Extinction

### Experimental results and theoretical interpretation

Luis W. Alvarez, Walter Alvarez, Frank Asaro, Helen V. Michel

In the 570-million-year period for which abundant fossil remains are available, there have been five great biological crises, during which many groups of organisms died out. The most recent of the great extinctions is used to define the boundary between the Cretaceous and Tertiary periods, about 65 million years

microscopic floating animals and plants; both the calcareous planktonic foraminifera and the calcareous nannoplankton were nearly exterminated, with only a few species surviving the crisis. On the other hand, some groups were little affected, including the land plants, crocodiles, snakes, mammals, and many kinds

**Summary.** Platinum metals are depleted in the earth's crust relative to their cosmic abundance; concentrations of these elements in deep-sea sediments may thus indicate influxes of extraterrestrial material. Deep-sea limestones exposed in Italy, Denmark, and New Zealand show iridium increases of about 30, 160, and 20 times, respectively, above the background level at precisely the time of the Cretaceous-Tertiary extinctions, 65 million years ago. Reasons are given to indicate that this iridium is of extraterrestrial origin, but did not come from a nearby supernova. A hypothesis is suggested which accounts for the extinctions and the iridium observations. Impact of a large earth-crossing asteroid would inject about 60 times the object's mass into the atmosphere as pulverized rock; a fraction of this dust would stay in the stratosphere for several years and be distributed worldwide. The resulting darkness would suppress photosynthesis, and the expected biological consequences match quite closely the extinctions observed in the paleontological record. One prediction of this hypothesis has been verified: the chemical composition of the boundary clay, which is thought to come from the stratospheric dust, is markedly different from that of clay mixed with the Cretaceous and Tertiary limestones, which are chemically similar to each other. Four different independent estimates of the diameter of the asteroid give values that lie in the range  $10 \pm 4$  kilometers.

ago. At this time, the marine reptiles, the flying reptiles, and both orders of dinosaurs died out (1), and extinctions occurred at various taxonomic levels among the marine invertebrates. Dramatic extinctions occurred among the

of invertebrates. Russell (2) concludes that about half of the genera living at that time perished during the extinction event.

Many hypotheses have been proposed to explain the Cretaceous-Tertiary (C-T)

extinctions (3, 4), and two recent meetings on the topic (5, 6) produced no sign of a consensus. Suggested causes include gradual or rapid changes in oceanographic, atmospheric, or climatic conditions (7) due to a random (8) or a cyclical (9) coincidence of causative factors; a magnetic reversal (10); a nearby supernova (11); and the flooding of the ocean surface by fresh water from a postulated arctic lake (12).

A major obstacle to determining the cause of the extinction is that virtually all the available information on events at the time of the crisis deals with biological changes seen in the paleontological record and is therefore inherently indirect. Little physical evidence is available, and it also is indirect. This includes variations in stable oxygen and carbon isotopic ratios across the boundary in pelagic sediments, which may reflect changes in temperature, salinity, oxygenation, and organic productivity of the ocean water, and which are not easy to interpret (13, 14). These isotopic changes are not particularly striking and, taken by themselves, would not suggest a dramatic crisis. Small changes in minor and trace element levels at the C-T boundary have been noted from limestone sections in Denmark and Italy (15), but these data also present interpretational difficulties. It is noteworthy that in pelagic marine sequences, where nearly continuous deposition is to be expected, the C-T boundary is commonly marked by a hiatus (3, 16).

In this article we present direct physical evidence for an unusual event at exactly the time of the extinctions in the planktonic realm. None of the current hypotheses adequately accounts for this evidence, but we have developed a hypothesis that appears to offer a satisfactory explanation for nearly all the available paleontological and physical evidence.

Luis Alvarez is professor emeritus of physics at Lawrence Berkeley Laboratory, University of California, Berkeley 94720. Walter Alvarez is an associate professor in the Department of Geology and Geophysics, University of California, Berkeley. Frank Asaro is a senior scientist and Helen Michel is a staff scientist in the Energy and Environment Division of Lawrence Berkeley Laboratory.

## Identification of Extraterrestrial Platinum Metals in Deep-Sea Sediments

This study began with the realization that the platinum group elements (platinum, iridium, osmium, and rhodium) are much less abundant in the earth's crust and upper mantle than they are in chondritic meteorites and average solar system material. Depletion of the platinum group elements in the earth's crust and upper mantle is probably the result of concentration of these elements in the earth's core.

Pettersson and Rotschi (17) and Goldschmidt (18) suggested that the low concentrations of platinum group elements in sedimentary rocks might come largely from meteoritic dust formed by ablation when meteorites passed through the atmosphere. Barker and Anders (19) showed that there was a correlation between sedimentation rate and iridium concentration, confirming the earlier suggestions. Subsequently, the method was used by Ganapathy, Brownlee, and Hodge (20) to demonstrate an extraterrestrial origin for silicate spherules in deep-sea sediments. Sarna-Wojcicki *et al.* (21) suggested that meteoritic dust accumulation in soil layers might enhance the abundance of iridium sufficiently to permit its use as a dating tool. Recently, Crocket and Kuo (22) reported iridium abundances in deep-sea sediments

and summarized other previous work.

Considerations of this type (23) prompted us to measure the iridium concentration in the 1-centimeter-thick clay layer that marks the C-T boundary in some sections in the Umbrian Apennines, in the hope of determining the length of time represented by that layer. Iridium can easily be determined at low levels by neutron activation analysis (NAA) (24) because of its large capture cross section for slow neutrons, and because some of the gamma rays given off during de-excitation of the decay product are not masked by other gamma rays. The other platinum group elements are more difficult to determine by NAA.

### Italian Stratigraphic Sections

Many aspects of earth history are best recorded in pelagic sedimentary rocks, which gradually accumulate in the relatively quiet waters of the deep sea as individual grains settle to the bottom. In the Umbrian Apennines of northern peninsular Italy there are exposures of pelagic sedimentary rocks representing the time from Early Jurassic to Oligocene, around 185 to 30 million years ago (25). The C-T boundary occurs within a portion of the sequence formed by pink limestone containing a variable amount of clay. This limestone, the *Scaglia ros-*

*sa*, has a matrix of coccoliths and coccolith fragments (calcite platelets, on the order of 1 micrometer in size, secreted by algae living in the surface waters) and a rich assemblage of foraminiferal tests (calcite shells, generally in the size range 0.1 to 2.0 millimeters, produced by single-celled animals that float in the surface waters).

In some Umbrian sections there is a hiatus in the sedimentary record across the C-T boundary, sometimes with signs of soft-sediment slumping. Where the sequence is apparently complete, foraminifera typical of the Upper Cretaceous (notably the genus *Globotruncana*) disappear abruptly and are replaced by the basal Tertiary foraminifer *Globigerina eugubina* (16, 26). This change is easy to recognize because *G. eugubina*, unlike the globotruncanids, is too small to see with the naked eye or the hand lens (Fig. 1). The coccoliths also show an abrupt change, with disappearance of Cretaceous forms, at exactly the same level as the foraminiferal change, although this was not recognized until more recently (27).

In well-exposed, complete sections there is a bed of clay about 1 cm thick between the highest Cretaceous and the lowest Tertiary limestone beds (28). This bed is free of primary  $\text{CaCO}_3$ , so there is no record of the biological changes during the time interval represented by the clay. The boundary is further marked by a zone in the uppermost Cretaceous in which the normally pink limestone is white in color. This zone is 0.3 to 1.0 meter thick, varying from section to section. Its lower boundary is a gradational color change; its upper boundary is abrupt and coincides with the faunal and floral extinctions. In one section (Contessa) we can see that the lower 5 mm of the boundary clay is gray and the upper 5 mm is red, thus placing the upper boundary of the zone in the middle of the clay layer.

The best known of the Umbrian sections is in the Bottaccione Gorge near Gubbio. Here some of the first work on the identification of foraminifera in thin section was carried out (29); the oldest known Tertiary foraminifer, *G. eugubina*, was recognized, named, and used to define the basal Tertiary biozone (16, 26); the geomagnetic reversal stratigraphy of the Upper Cretaceous and Paleocene was established, correlated to the marine magnetic anomaly sequence, and dated with foraminifera (30); and the extinction of most of the nannoplankton was shown to be synchronous with the disappearance of the genus *Globotruncana* (27).

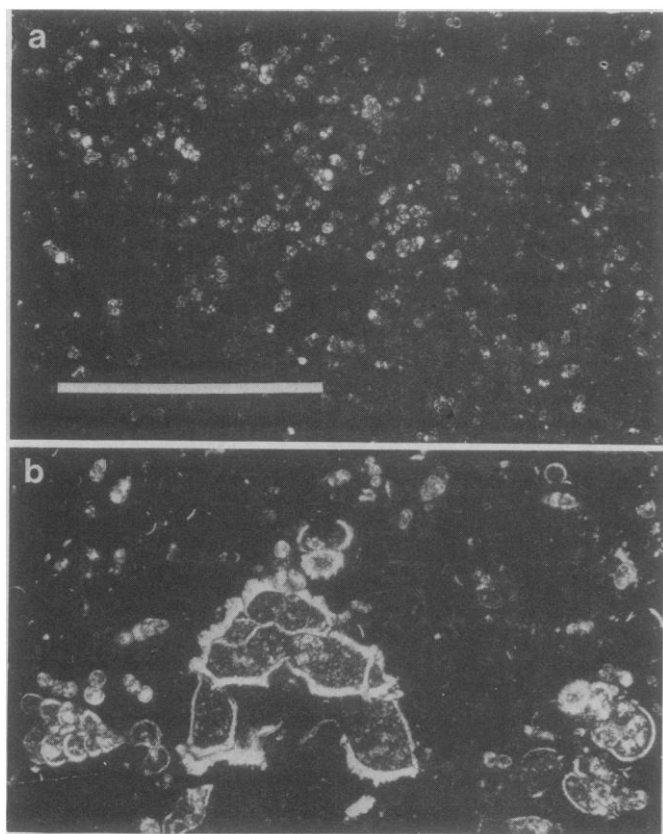


Fig. 1. Photomicrographs of (a) the basal bed of the Tertiary, showing *Globigerina eugubina*, and (b) the top bed of the Cretaceous, in which the largest foraminifer is *Globotruncana contusa*. Both sections are from the Bottaccione section at Gubbio; they are shown at the same scale and the bar in (a) is 1 mm long.

## Results from the Italian Sections

Our first experiments involved NAA of nine samples from the Bottaccione section (two limestone samples from immediately above and below the boundary plus seven limestone samples spaced over 325 m of the Cretaceous). This was supplemented by three samples from the nearby Contessa section (two from the boundary clay and one from the basal Tertiary bed). Stratigraphic positions of these samples are shown in Fig. 2.

Twenty-eight elements were selected for study because of their favorable nuclear properties, especially neutron capture cross sections, half-lives, and gamma-ray energies. The results of these analyses are presented in Fig. 3 on a logarithmic plot to facilitate comparison of the relative changes in elements over a wide range of concentrations. The only preparation given to these samples was removal of the  $\text{CaCO}_3$  fraction by dissolution in dilute nitric acid. Figure 3 shows elemental abundances as gram of element per gram of insoluble clay residue. The limestones generally contain about 5 percent clay. The boundary clay layer contains about 50 percent  $\text{CaCO}_3$ , but this is coarse-grained calcite that probably crystallized during deformation long after deposition. Chemical yields of iridium in the acid-insoluble fraction averaged 44 percent for the red and gray Contessa boundary clays, and this value was assumed for all the other samples.

Twenty-seven of the 28 elements show very similar patterns of abundance variation, but iridium shows a grossly different behavior; it increases by a factor of about 30 in coincidence with the C-T boundary, whereas none of the other elements as much as doubles with respect to an "average behavior" shown in the lower right panel of Fig. 3. Figure 4 shows a typical gamma-ray spectrum used to measure the Ir abundance, 5.5 parts per billion (ppb).

In follow-up experiments we analyzed five more samples from the Bottaccione section, eight from Gorgo a Cerbara (28 kilometers north of Gubbio), and four large samples of the boundary clay from the two sections near Gubbio and two sections about 30 km to the north (31). The chemical yield of iridium in the acid-insoluble fraction was  $95 \pm 5$  percent for the Contessa boundary clay, and a 100 percent yield was assumed for all the other samples.

Figure 5 shows the results of 29 Ir analyses completed on Italian samples. Note that the section is enlarged and that the scale is linear in the vicinity of the C-T boundary, where details are important,

but changes to logarithmic to show results from 350 m below to 50 m above the boundary. It is also important to note that analyses from five stratigraphic sections are plotted on the same diagram on the basis of their stratigraphic position above or below the boundary. Because slight differences in sedimentation rate probably exist from one section to the next, the chronologic sequence of samples from different sections may not be exactly correct. Nevertheless, Fig. 5

gives a clear picture of the general trend of iridium concentrations as a function of stratigraphic level.

The pattern, based especially on the samples from the Bottaccione Gorge and Gorgo a Cerbara, shows a steady background level of  $\sim 0.3$  ppb throughout the Upper Cretaceous, continuing into the uppermost bed of the Cretaceous. The background level in the acid-insoluble residues is roughly comparable to the iridium abundance measured by other

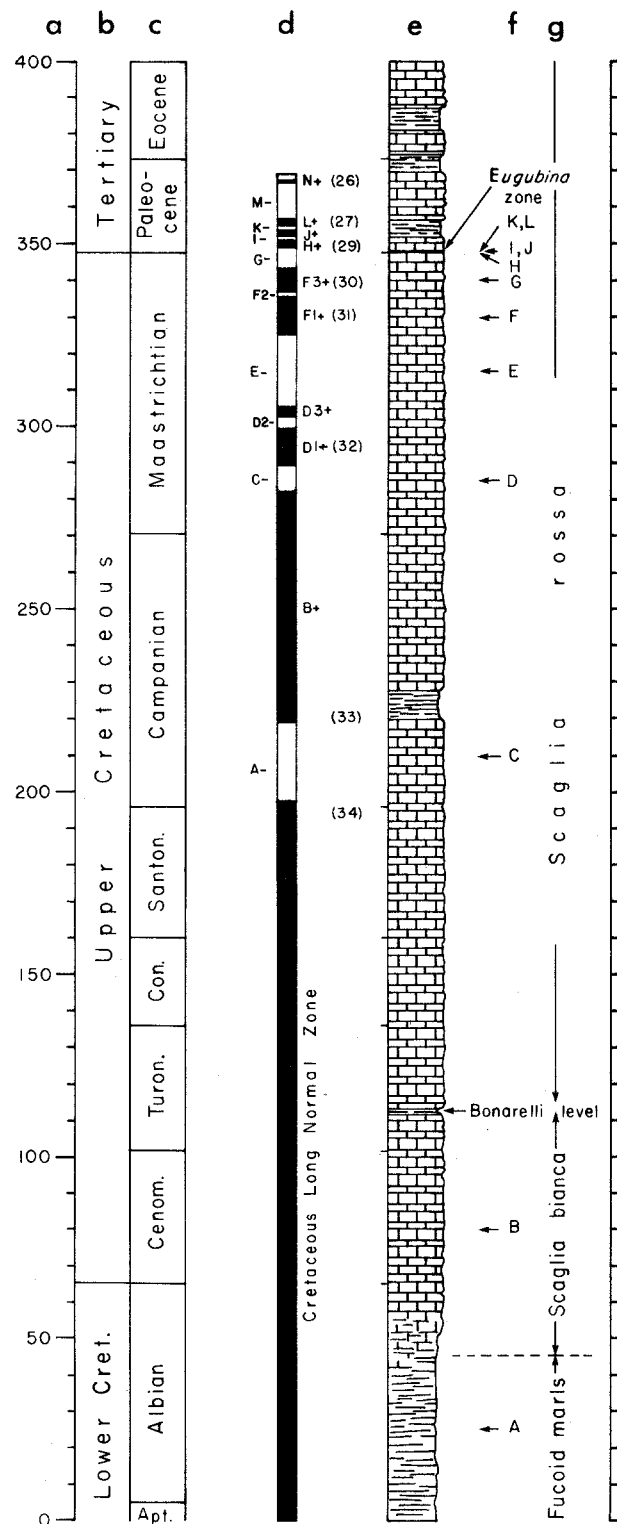


Fig. 2. Stratigraphic section at the Bottaccione Gorge, Gubbio (30). (a) Meter levels. (b) Systems. (c) Stages. (d) Magnetic polarity zones (black is normal, white is reversed polarity, letters give Gubbio polarity zonation, numbers are equivalent marine magnetic anomalies). (e) Lithology. (f) Samples used in first NAA study (samples I, J, and L are from equivalent positions in the Contessa section, 2 km to the northwest). (g) Formation names.



workers (19, 22, 32) in deep-sea clay sediments. This level increases abruptly, by a factor of more than 30, to 9.1 ppb, the Ir abundance in the red clay from the Contessa section. Iridium levels are high in clay residues from the first few beds of Tertiary limestone, but fall off to background levels by 1 m above the boundary. For comparison, the upper dashed line in Fig. 5 shows an exponential decay from the boundary clay Ir level with a half-height of 4.6 cm.

To test the possibility that iridium might somehow be concentrated in clay layers, we subsequently analyzed two red clay samples from a short distance below the C-T boundary in the Bottaccione section. One is from a distinctive clay layer 5 to 6 mm thick, 1.73 m below the boundary; the other is from a 1- to 2-mm bedding-plane clay seam 0.85 m below the boundary. The whole-rock analyses of these clays showed no detectable Ir with limits of 0.5 and 0.24 ppb, respectively. Thus neither clay layers from below the C-T boundary nor clay components in the limestone show evidence of Ir above the background level.

## The Danish Section

To test whether the iridium anomaly is a local Italian feature, it was desirable to analyze sediments of similar age from another region. The sea cliff of Stevns Klint, about 50 km south of Copenhagen, is a classical area for the C-T boundary and for the Danian or basal stage of the Tertiary. A collection of up-to-date papers on this and nearby areas has recently been published, which includes a full bibliography of earlier works (6, vol. 1).

Our samples were taken at Højerup Church (33). At this locality the Maastrichtian, or uppermost Cretaceous, is represented by white chalk containing black chert nodules in undulating layers with amplitudes of a few meters and wavelengths of 10 to 50 m (14). These undulations are considered to represent bryozoan banks (34). The C-T boundary is marked by the *Fiskeler*, or fish clay, which is up to 35 cm thick in the deepest parts of the basins between bryozoan banks (14) but commonly only a few centimeters thick, thinning or disappearing, over the tops of the banks. The fish clay

at Højerup Church was studied in detail by Christensen *et al.* (14), who subdivided it into four thin layers; we analyzed a sample mixing the two internal layers (units III and IV of Christensen *et al.*). These layers are black or dark gray, and the lower one contains pyrite concretions; the layers below and above (II and V) are light gray in color. Undisturbed lamination in bed IV suggests that no bottom fauna was present during its deposition (14). Above the fish clay, the *Cerithium* limestone is present to a thickness of about 50 cm in the small basins, disappearing over the banks. It is hard, yellowish in color, and cut by abundant burrows. Above this is a thick bryozoan limestone.

The presence of a thin clay layer at the C-T boundary in both the Italian and Danish sections is quite striking. However, there are notable differences as well. The Danish sequence was clearly deposited in shallower water (35), and the Danish limestones preserve an extensive bottom-dwelling fauna of bivalves (36), echinoderms (37), bryozoans (38), and corals (39).

Foraminiferal (40) and coccolith (41)

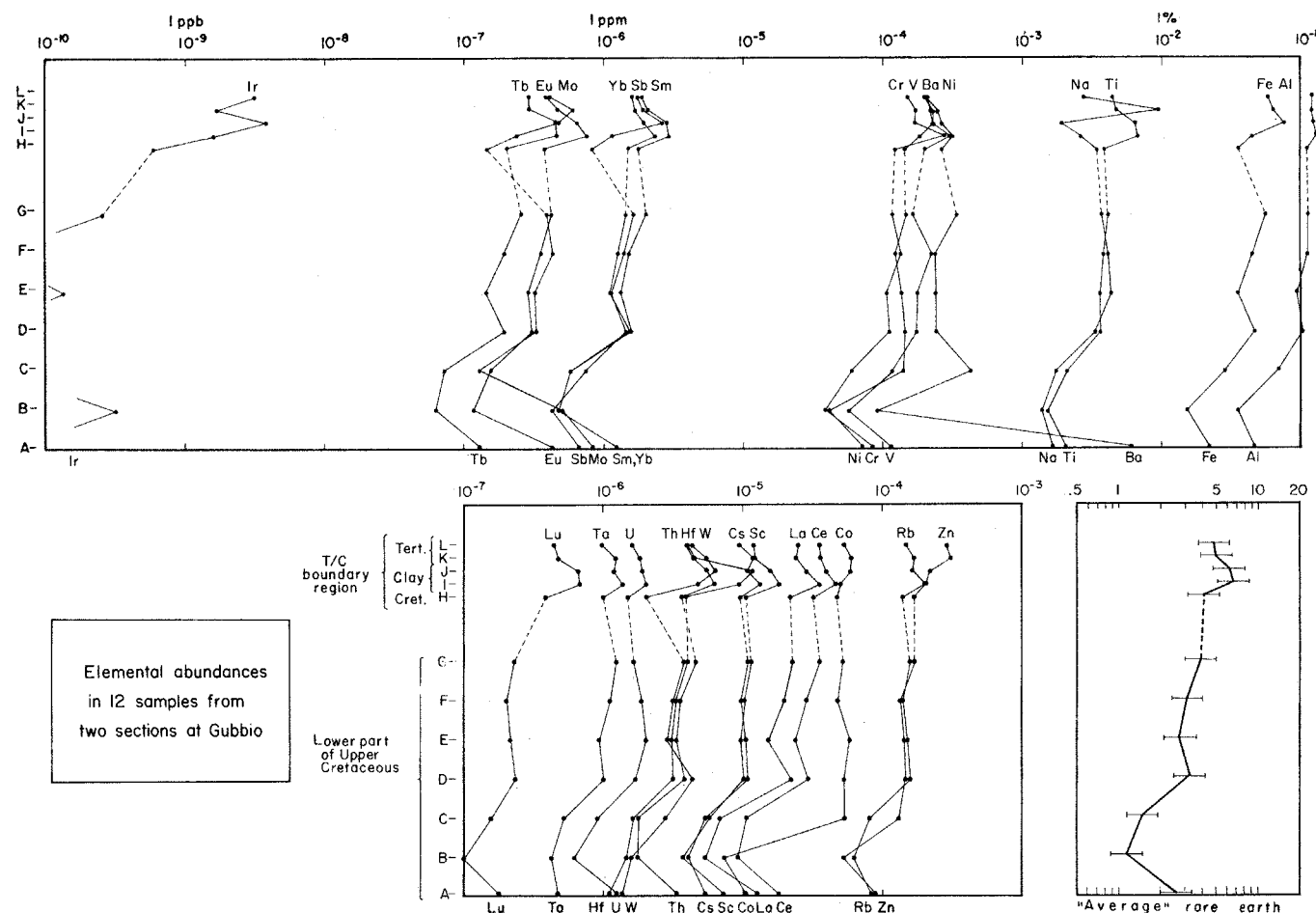


Fig. 3. Abundance variations of 28 elements in 12 samples from two Gubbio sections. Flags on "average rare earth" diagram are  $\pm 30$  percent and include all rare earth data.

zonation indicates that the C-T boundaries at Gubbio and Stevns Klint are at least approximately contemporaneous, and they may well be exactly synchronous. However, no paleomagnetic results are available from Stevns Klint, so synchronicity cannot be tested by reversal stratigraphy.

## Results from the Danish Section

Seven samples were taken from near the C-T boundary (Fig. 6). Fractions of each sample were treated with dilute nitric acid, and the residues were filtered, washed, and heated to 800°C. The yield of acid-insoluble residue was 44.5 percent for the boundary fish clay and varied from 0.62 to 3.3 percent for the pelagic limestones (Table 1).

Neutron activation analysis (24) and x-ray fluorescence (XRF) (42, 43) measurements were made on all seven samples both before and after the acid treatment. This measurement regime was more sophisticated than that used for the Italian sections studied earlier, and 48 elements were determined.

The Cretaceous and Tertiary acid-insoluble residues were each rather homogeneous in all of the measured elements, and the two groups were only slightly different from each other. The residue from the clay boundary layer was much different in composition (Figs. 7 and 8 and Table 2), and this suggested a different source for the boundary clay.

As shown in Table 1, the Ir in the boundary layer residue rises by about a factor of 160 over the background level (~0.26 ppb). A 1-cm thickness of this layer would have about  $72 \times 10^{-9}$  gram of Ir per square centimeter. To test whether there is enough Ir in the seawater to contribute to this value, we made a measurement of the Ir in the ocean off the central California coast. In water passed through a 0.45- $\mu$ m filter Ir was undetected, giving an upper limit of  $4 \times 10^{-13}$  g of Ir per gram of seawater. If the depth of the shallow ancient Danish sea is assumed to be less than 100 m and our limit for Ir in seawater is applicable, then the maximum Ir in the 100-m column of water should be  $4 \times 10^{-9}$  g/cm<sup>2</sup>, almost a factor of 20 lower than the observed value. So there was probably not enough Ir stored in the seawater to explain the amount observed in the Danish boundary. Iridium has apparently not been detected in seawater. One tabulated result (44) contains a typographical error that places the value for indium in

the atomic number position of iridium. Iridium has been detected (45) in a warm spring on Mount Hood in northern California at a level of  $7 \times 10^{-12}$  g per gram of water, and in two cold-water sources at levels of  $3 \times 10^{-13}$  to  $4 \times 10^{-13}$  g per gram of water. Many other cold-water sources in this area had Ir levels less than  $1 \times 10^{-13}$  g/g.

## The Boundary Layers

The whole-rock composition of the Contessa boundary layer (a mixture of red and gray clay) is shown in Table 3. There are two recognizable sublayers, each about 0.5 cm thick, the upper being red in color and the lower gray. The elemental iron content, which may explain

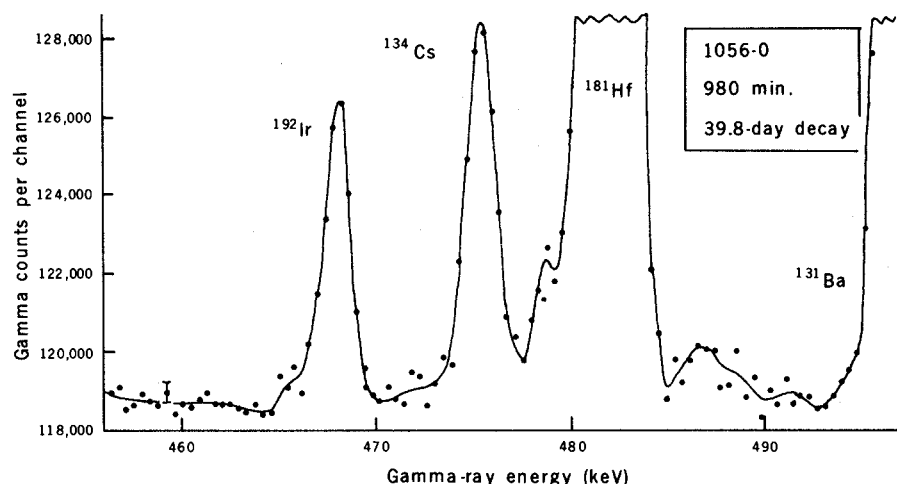
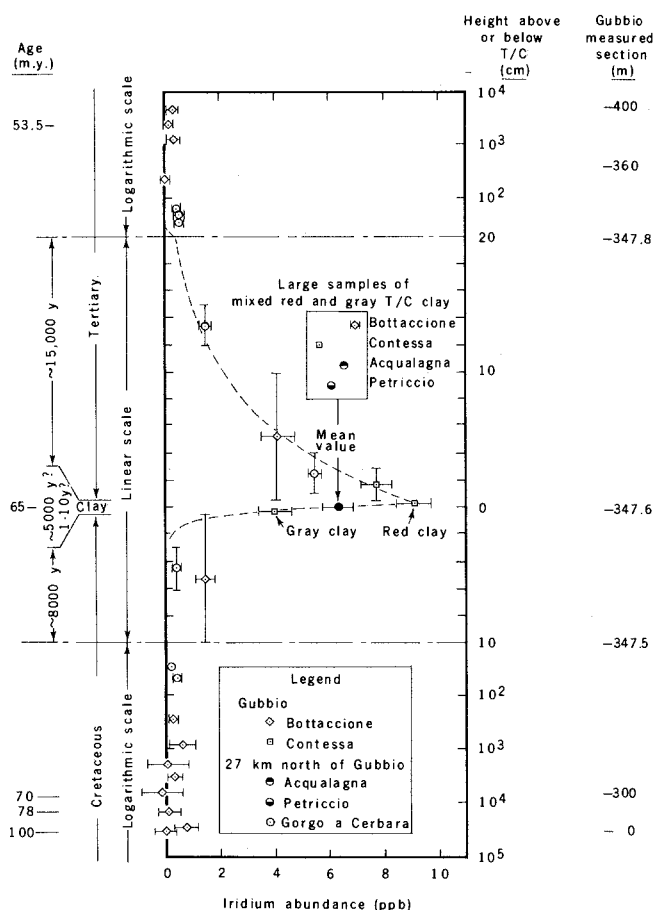


Fig. 4. Typical gamma-ray spectrum used to determine Ir abundance (5.5 ppb) in nitric acid-insoluble residues without further chemistry. Note that the entire spectrum rests on a background of 118,000 counts. Detector volume was 128 cm<sup>3</sup>; length of count was 980 minutes. Count began 39.8 days after the end of the irradiation. Residue is from a Tertiary limestone sample taken 2.5 cm above the boundary at Gorgo a Cerbara (see Fig. 5).

Fig. 5. Iridium abundances per unit weight of 2N HNO<sub>3</sub> acid-insoluble residues from Italian limestones near the Tertiary - Cretaceous boundary. Error bars on abundances are the standard deviations in counting radioactivity. Error bars on stratigraphic position indicate the stratigraphic thickness of the sample. The dashed line above the boundary is an "eyeball fit" exponential with a half-height of 4.6 cm. The dashed line below the boundary is a best fit exponential (two points) with a half-height of 0.43 cm. The filled circle and error bar are the mean and standard deviation of Ir abundances in four large samples of boundary clay from different locations.



the color, is significantly higher in the residue of the red layer (7.7 versus 4.5 percent) than in the gray, and so is the Ir ( $9.1 \pm 0.6$  versus  $4.0 \pm 0.6$  ppb). Boundary samples were analyzed from the Bottaccione Gorge nearby and two other areas about 30 km to the north.

In samples taken near the Italian boundary layer, the chemical compositions of all clay fractions were roughly the same except for the element Ir. However, there are discernible differences, as shown in Fig. 9, which suggest that at least part of the boundary layer clay had a different origin than the Cretaceous and Tertiary clays.

The Danish C-T boundary clay is somewhat thicker than 1 cm and is divided into four layers, as mentioned earlier. Only a single mixed sample from the two middle layers was measured, so no information is available on the chemical variations within the boundary. The average Ir abundance is 29 ppb in the whole rock or 65 ppb based on the weight of acid-insoluble residue.

The whole-rock abundances and mineral composition of the Danish boundary clay are shown in Table 3, and the abundances of pertinent trace elements are shown in Table 2. The major silicate minerals that must be present were not detected, so the other mineral abundances were normalized to give the amount of

Table 1. Abundance of iridium in acid-insoluble residues in the Danish section.

Sample*	Abundance of iridium (ppb)	Abundance† of acid-insoluble residues (%)
SK, +2.7 m	< 0.3	3.27
SK, +1.2 m	< 0.3	1.08
SK, +0.7 m	$0.36 \pm 0.06$	0.836
Boundary	$41.6 \pm 1.8\ddagger$	44.5
SK, -0.5 m	$0.73 \pm 0.08$	0.654
SK, -2.2 m	$0.25 \pm 0.08$	0.621
SK, -5.4 m	$0.30 \pm 0.16$	0.774

\*Numerical values are the distances above (+) or below (-) the boundary layer; SK, Stevns Klint. †The boundary layer has a much higher proportion of clay than the pelagic limestones above and below. ‡Some iridium dissolved in the nitric acid. The whole-rock abundance was  $28.6 \pm 1.3$  ppb.

calcite expected from the calcium measurement. The boundary clay fraction is far different chemically from the limestone clay fractions above and below, which are similar to each other. Pyrite is present in the boundary clay, and elements that form water-insoluble sulfides are greatly enhanced in this layer. The trace elements that are depleted are those that often appear as clay components. The element magnesium is an

exception. Its enhancement may be due to replacement of iron in the clay lattices in the sulfide environment or to a different, more mafic source for the boundary layer clay than for the Tertiary and Cretaceous clays.

Recent unpublished work by D. A. Russell of the National Museums of Canada and by the present authors has shown that the boundary layer whole-rock concentration of Ir in a section near Woodside Creek, New Zealand, is approximately 20 times the average concentration in the adjacent Cretaceous and Tertiary limestones.

## A Sudden Influx of Extraterrestrial

### Material

To test whether the anomalous iridium at the C-T boundary in the Gubbio sections is of extraterrestrial origin, we considered the increases in 27 of the 28 elements measured by NAA that would be expected if the iridium in excess of the background level came from a source with the average composition of the earth's crust. The crustal Ir abundance, less than 0.1 ppb (19, 22), is too small to be a worldwide source for material with an Ir abundance of 6.3 ppb, as found near Gubbio. Extraterrestrial sources with Ir levels of hundreds of parts per

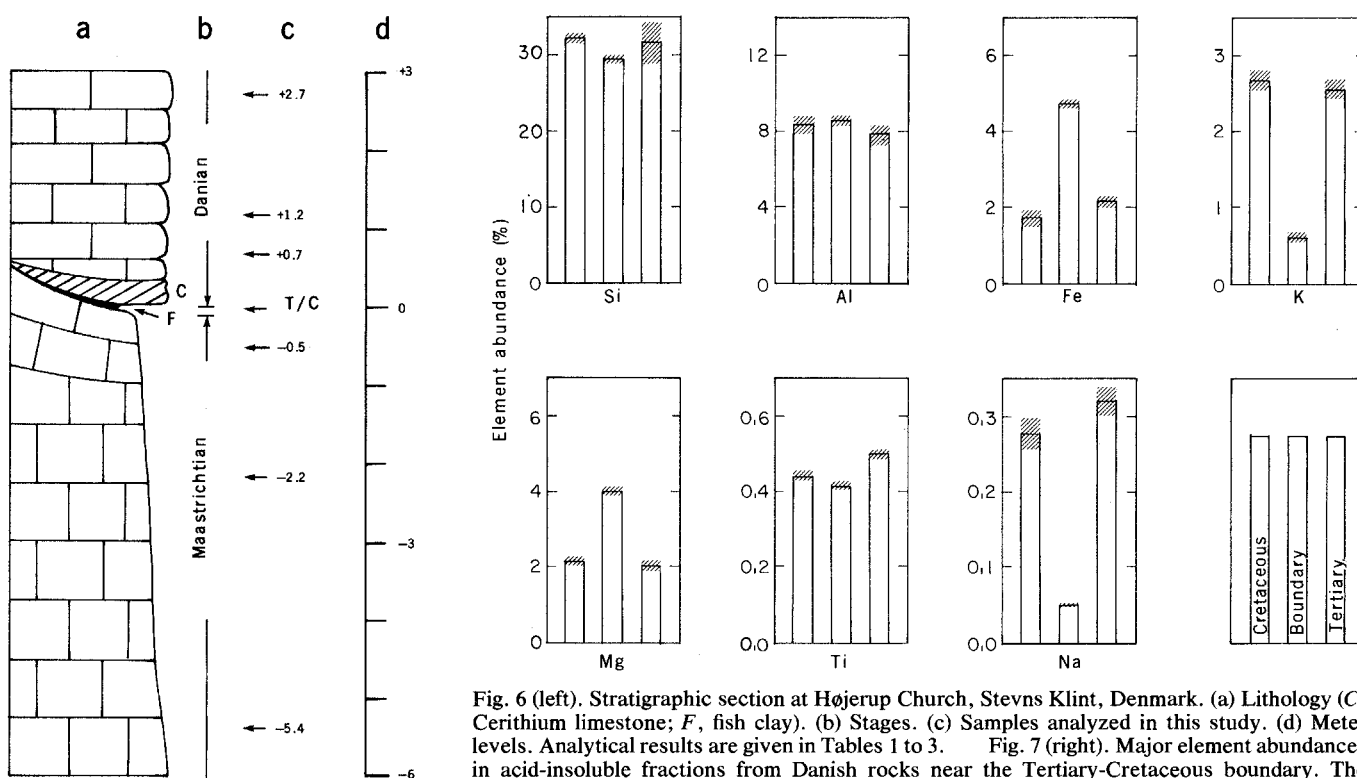


Fig. 6 (left). Stratigraphic section at Højerup Church, Stevns Klint, Denmark. (a) Lithology (C, Cerithium limestone; F, fish clay). (b) Stages. (c) Samples analyzed in this study. (d) Meter levels. Analytical results are given in Tables 1 to 3. Fig. 7 (right). Major element abundances in acid-insoluble fractions from Danish rocks near the Tertiary-Cretaceous boundary. The crosshatched areas for the Cretaceous and Tertiary values each represent root-mean-square deviations for three samples. (Only two measurements of magnesium and silicon were included in the Cretaceous values.) For the boundary layer sample the crosshatched areas are the standard deviations associated with counting errors. Measurements of silicon and magnesium were done by XRF (42), all others were by NAA.

billion or higher are more likely to have produced the Ir anomaly. Figure 10 shows that if the source had an average earth's crust composition (46), increases significantly above those observed would be expected in all 27 elements. However, for a source with average carbonaceous chondrite composition (46), only nickel should show an elemental increase greater than that observed. As shown in Fig. 11, such an increase in nickel was not observed, but the predicted effect is small and, given appropriate conditions, nickel oxide would dissolve in seawater (47). We conclude that the pattern of elemental abundances in the Gubbio sections is compatible with an extraterrestrial source for the anomalous iridium and incompatible with a crustal source.

The Danish boundary layer, which has much more Ir than the Italian C-T clay, is even less likely to have had a crustal origin. Rocks from the upper mantle (which has more Ir than the crust) have less than 20 ppb (48) and are therefore an unlikely worldwide source. There are, however, localized terrestrial sources with much higher Ir abundances; for example, nickel sulfide and chromite ores (48) have Ir levels of hundreds and thousands of parts per billion, respectively. The Danish boundary layer, however, does not have enough nickel [506 parts per million (ppm)] or chromium (165

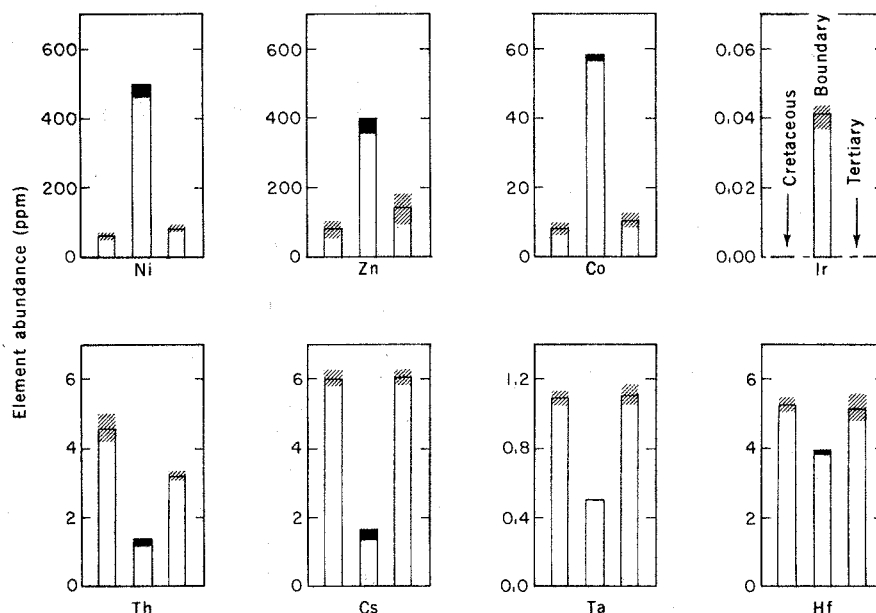


Fig. 8. Selected trace element abundances of Danish acid-insoluble residues. First bar is the mean value [root-mean-square deviation (RMSD) is shown by the crosshatched areas] for the given element in the three Cretaceous residues. Second bar is the abundance (counting error is shown by solid areas) for the given element in the boundary layer residue. Third bar is the mean value and RMSD for the given element in the three Tertiary residues. Measurements were by NAA, except for zinc, which was measured by XRF (43). Significant amounts of nickel, zinc, cobalt, iridium, and thorium in all samples dissolved in the 2N HNO<sub>3</sub>. Very little cesium, tantalum, or hafnium in any of the samples dissolved in the acid.

ppm) to explain its Ir in this fashion, unless the marine chemistry concentrated Ir preferentially (even in the sulfide environment) and disposed of the other elements elsewhere. The probability of

these effects occurring worldwide seems less likely than an extraterrestrial origin for the Ir.

We next consider whether the Ir anomaly is due to an abnormal influx of

Table 2. Abundance of trace elements in the Danish boundary layer (parts per million).

Element	(1) Abundance in whole rock/ abundance of residue*	(2) Abundance in residue*	Element	(1) Abundance in whole rock/ abundance of residue	(2) Abundance in residue
<i>Enhanced elements†</i>			<i>Depleted elements</i>		
V	391 ± 27	330 ± 31	Mn	102.0 ± 1.3	21.3 ± 0.5
Cr	371 ± 13	358 ± 9	Rb	27 ± 7	35 ± 4
Co	141.6 ± 1.8	57.2 ± 0.7	Y‡	79 ± 6	6.3 ± 1.8
Ni	1137 ± 31	479 ± 14	Zr‡	144 ± 11	125 ± 6
Cu‡	167 ± 14	93 ± 6	Nb‡	8 ± 4	6.1 ± 1.8
Zn‡	1027 ± 49	378 ± 18	Cs	1.87 ± 0.19	1.51 ± 0.14
As	96 ± 8	68 ± 4	La	61.1 ± 1.6	6.8 ± 0.4
Se§	46.5 ± 0.6	12.1 ± 0.3	Ce	57.0 ± 1.2	9.7 ± 0.6
Mo	29.0 ± 2.5	20.3 ± 1.4	Nd	63.4 ± 2.7	5.4 ± 0.6
Ag§	2.6 ± 0.9	3.5 ± 0.7	Sm	11.93 ± 0.08	0.781 ± 0.008
In§	0.245 ± 0.022	0.086 ± 0.019	Eu	2.76 ± 0.11	0.121 ± 0.010
Sb	8.0 ± 0.4	6.7 ± 0.4	Tb	1.84 ± 0.04	0.148 ± 0.014
Ba	1175 ± 16	747 ± 11	Dy	11.24 ± 0.12	0.908 ± 0.033
Ir	0.0643 ± 0.0029	0.0416 ± 0.0018	Yb	5.02 ± 0.09	0.56 ± 0.05
Pb‡	64 ± 14	28 ± 7	Lu	0.553 ± 0.031	0.083 ± 0.004
<i>Other elements†</i>			Hf	4.34 ± 0.16	3.88 ± 0.07
Sc	20.74 ± 0.16	14.30 ± 0.14	Ta	0.508 ± 0.011	0.500 ± 0.005
Ga‡	30 ± 6	19.8 ± 3.0	Th	7.1 ± 0.4	1.28 ± 0.06
Sr‡	1465 ± 72	48.1 ± 2.4	U	8.63 ± 0.09	0.918 ± 0.024
Au	< 0.12	0.027 ± 0.007			

\*Column 1 minus column 2 is the amount of an element that dissolved in the acid or was lost in the firing; abundance of residue = 44.5 percent. †Elements V, Ag, and In are at least 20 percent and all other "enhanced elements" are at least a factor of 3 more abundant in the boundary residue than in the other residues. All "depleted elements" are at least 20 percent less abundant in the boundary residue than in the other residues. "Other elements" do not show a consistent pattern of boundary residue abundances relative to the others. ‡Measured by hard XRF (43). §Flux monitors were used in the NAA measurements of these elements. The indicated errors are applicable for comparing the two entries for a given element, but calibration uncertainties of possibly 10 to 20 percent must be considered when the values are used for other purposes.



extraterrestrial material at the time of the extinctions, or whether it was formed by the normal, slow accumulation of meteoritic material (19), followed by concentration in the boundary rocks by some identifiable mechanism.

There is *prima facie* evidence for an abnormal influx in the observations that the excess iridium occurs exactly at the time of one of the extinctions; that the extinctions were extraordinary events, which may well indicate an extraordinary cause; that the extinctions were clearly worldwide; and that the iridium anomaly is now known from two different areas in western Europe and in New Zealand. Furthermore, we will show in a later section that impact of a 10-km earth-crossing asteroid, an event that probably occurs with about the same frequency as major extinctions, may have produced the observed physical and biological effects. Nevertheless, one can invent two other scenarios that might lead

to concentration of normal background iridium at the boundary. These appear to be much less likely than the sudden-influx model, but we cannot definitely rule out either one at present.

The first scenario requires a physical or chemical change in the ocean waters at the time of the extinctions, leading to extraction of iridium resident in the seawater. This would require iridium concentrations in seawater that are higher than those presently observed. In addition, it suggests that the positive iridium anomaly should be accompanied by a compensating negative anomaly immediately above, but this is not seen.

The second scenario postulates a reduction in the deposition rate of all components of the pelagic sediment except for the meteoritic dust that carries the concentrated iridium. This scenario requires removal of clay but not of iridium-bearing particles, perhaps by currents of exactly the right velocity. These currents

must have affected both the Italian and Danish areas at exactly the time of the C-T extinctions, but at none of the other times represented by our samples. We feel that this scenario is too contrived, a conclusion that is justified in more detail elsewhere (23).

In summary, we conclude that the anomalous iridium concentration at the C-T boundary is best interpreted as indicating an abnormal influx of extraterrestrial material.

### Negative Results of Tests for the Supernova Hypothesis

Considerable attention has been given to the hypothesis that the C-T extinctions were the result of a nearby supernova (11). A rough calculation of the distance from the assumed supernova to the solar system, using the measured surface density of iridium in the Gubbio

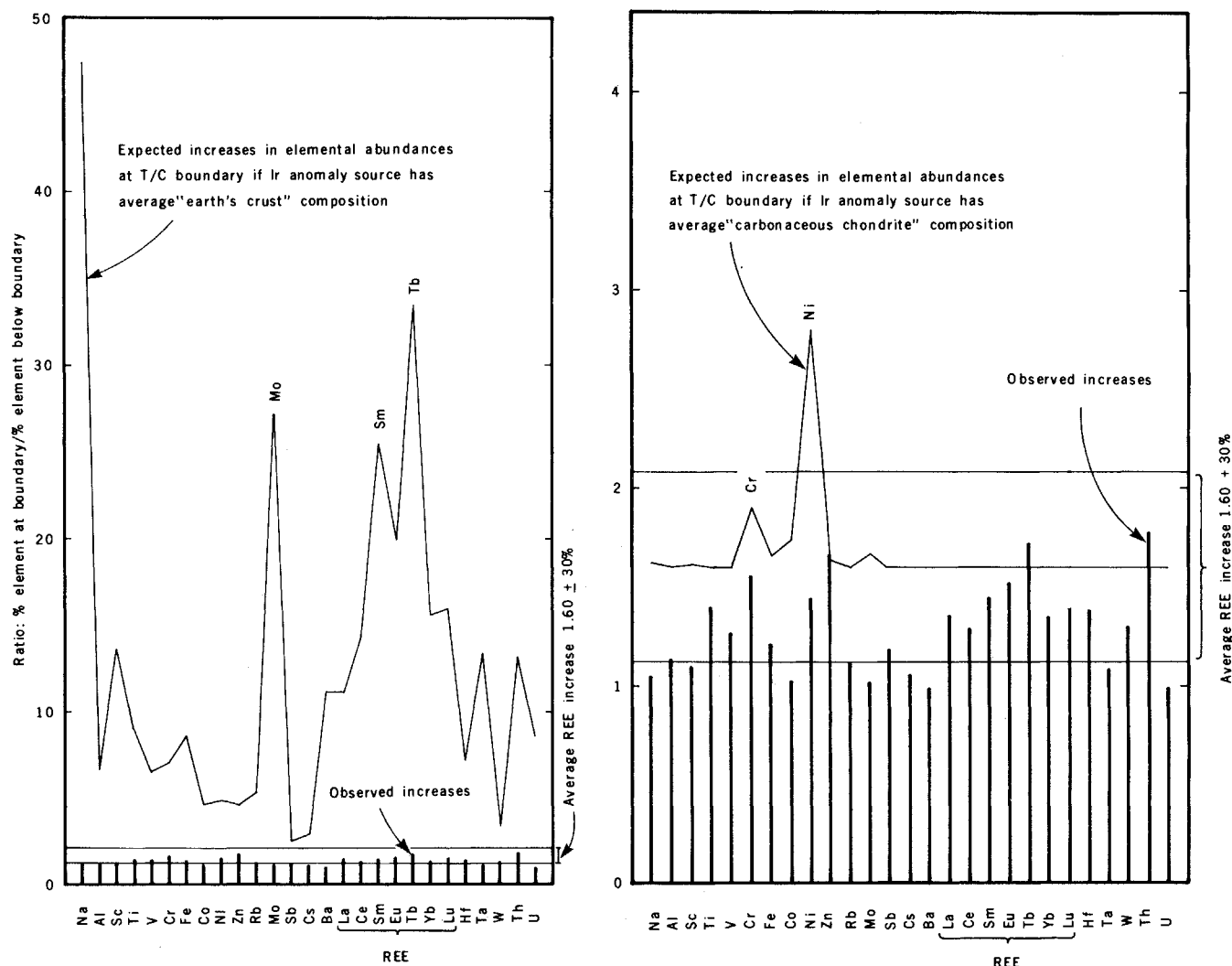


Fig. 10 (left). Comparison of observed elemental abundance patterns in the Gubbio section samples with average patterns expected for crustal material (46). Fig. 11 (right). Comparison of observed elemental abundance patterns in the Gubbio section samples with patterns expected for carbonaceous chondrites (46).

boundary layer and the amount of iridium expected to be blown off in the supernova explosion, gives about 0.1 light-year. The probability is about  $10^{-9}$  (49) that, during the last 100 million years, a supernova occurred within this distance from the sun. Any mechanism with such a low a priori probability is obviously a one-time-only theory. Nevertheless, because the theory could be subjected to direct experimental tests, it was treated as a real possibility until we obtained two other independent pieces of evidence that forced us to reject it.

Elements heavier than nickel can be produced in stars only by neutron capture followed by beta decay. The most intense source of neutrons so far postulated is that produced by the gravitational collapse of the core of a star that leads immediately to a supernova explosion. In this environment the rapid capture of neutrons ("r process") leads to the formation of the heaviest known isotopes. The slower capture of neutrons by heavy isotopes in highly evolved stars ("s process") leads to a different mix of isotopes (50).

One heavy isotope in particular offered the possibility of testing the supernova hypothesis; this is  $^{244}\text{Pu}$ , with a half-life of  $80.5 \times 10^6$  years. The explosion of a supernova should send out an expanding shell of newly created heavy elements, with a ratio of Ir atoms to  $^{244}\text{Pu}$  atoms equal to about  $10^3$ . This value is inferred from the existence of an anomaly in the meteoritic abundance of heavy xenon isotopes that is interpreted as being due to the fission of  $^{244}\text{Pu}$  (51). Any  $^{244}\text{Pu}$  incorporated in the earth at the time of the creation of the solar system, about 4.7 billion years ago, would have decayed by 58 half-lives, or by a factor of  $10^{17}$ , which would make it quite undetectable in the Gubbio section by the most sensitive techniques available. If the C-T extinctions were due to a supernova, and if this were the source of the anomalous Ir, each Ir atom should have been accompanied by about  $10^{-3}$   $^{244}\text{Pu}$  atom, and this  $^{244}\text{Pu}$  would have decayed by only a factor of 2.

Plutonium-244 is easily detected both by mass spectrometry and by NAA. The former is more sensitive, but the latter was immediately available. In NAA, which we utilized,  $^{244}\text{Pu}$  is converted to  $^{245}\text{Pu}$ , which has a half-life of 10 hours and emits many characteristic gamma rays and x-rays. Plutonium was chemically separated from 25- and 50-g batches of boundary clay and from a 50-g batch of bedding clay from below the C-T boundary, and nearly "mass-free"

samples were obtained—no carriers were added. Chemical separations were also performed on the plutonium fraction after the neutron irradiation. No significant gamma radiation was observed, other than that associated with the plutonium isotopes. In order to measure our chemical yields, Gubbio acid-soluble and acid-insoluble residues were spiked with small amounts of  $^{238}\text{Pu}$  tracer. This plutonium isotope is easily detectable through its alpha decay, as its half-life is only 87.7 years. In addition, one of the samples was spiked with  $^{244}\text{Pu}$ . Figure 12a shows the gamma-ray spectrum of the

sample spiked with about 20 picograms of  $^{244}\text{Pu}$ ; it indicates both the sensitivity of NAA for the detection of  $^{244}\text{Pu}$  and the freedom of the purified sample from other elements that might interfere with the detection of  $^{244}\text{Pu}$ . The plutonium isotopic ratios in this sample and in the tracer were also measured with a single-direction-focusing mass spectrometer 5 feet in radius.

No  $^{244}\text{Pu}$  was detected in the Gubbio samples (Fig. 12b), with a detection limit of less than 10 percent of the amount that would be expected to accompany the measured iridium if a supernova were re-

Fig. 9. Some of the element abundances measured in acid-insoluble residues of Cretaceous, boundary layer, and Tertiary rocks near Gubbio. Data include all samples from that area measured within 19 m of the boundary. There were four samples from each of the three layers; the crosshatched areas are the standard deviations. The abundance patterns for samples from ~27 km north of Gubbio are similar to those shown.

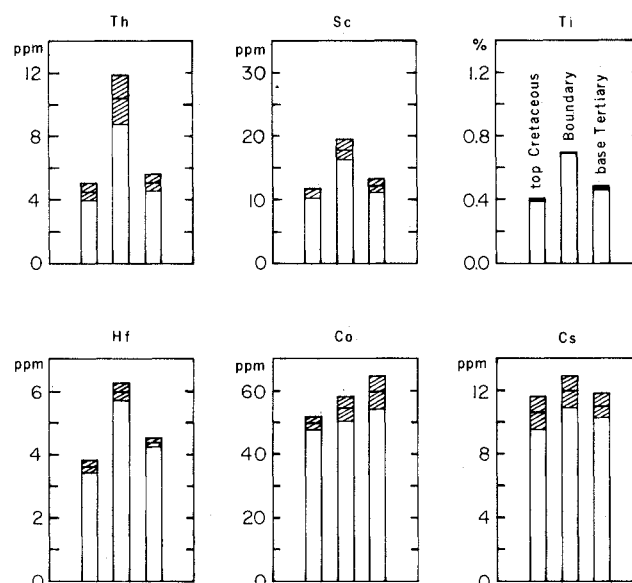


Table 3. Whole-rock composition of the Gubbio and Danish boundary layers (percent).

Element* or mineral	Abundance in boundary layer†		
	Gubbio (Contessa) measured	Denmark	
		Measured	Normalized
SiO <sub>2</sub>	27.7 ± 0.6	29.0 ± 0.6	
Al <sub>2</sub> O <sub>3</sub>	12.19 ± 0.15	8.01 ± 0.17	
FeO‡	4.53 ± 0.05	4.35 ± 0.04	
MgO	1.10 ± 0.07	3.07 ± 0.10	
CaO	22.6 ± 0.4	23.1 ± 0.4	
Na <sub>2</sub> O	0.1806 ± 0.0036	0.0888 ± 0.0018	
K <sub>2</sub> O	2.46 ± 0.20	0.38 ± 0.04	
TiO <sub>2</sub>	0.521 ± 0.022	0.324 ± 0.016	
S <sup>2-</sup>	Not detected	~ 1.1	
PO <sub>4</sub> <sup>3-</sup>	Not detected	0.92 ± 0.09	
CO <sub>2</sub> §	17.7 ± 0.3	18.4 ± 0.3	
Σ Trace elements	~ 0.2	~ 0.3	
Sum	89.2 ± 0.8	90.3 ± 1.0	
Difference	10.8 ± 0.8	9.7 ± 1.0	
Calcite		~ 90	41.5 (norm)
Quartz		5-7	~ 3
Pyrite		~ 5	~ 2
Illite		2-3	~ 1

\*Abundance values are for element expressed as form shown. †Elements Si, Ca, Mg, S, P, and Gubbio Ti were measured by soft XRF (42). Some S may be lost in this sample preparation procedure. The Denmark Ti was measured by hard XRF (43). All other measurements were by NAA. Mineral analyses were done by M. Ghorso and I. S. E. Carmichael by x-ray diffraction. ‡Total Fe expressed as FeO. §The CO<sub>2</sub> abundance was calculated from the Ca abundance by assuming all Ca was present as the carbonate. ||The difference is mainly water and organic material.

sponsible for the latter. The ocean, however, can produce chemical and physical changes in depositing materials as well as diagenetic alterations in the deposited sediments, so the absence of measurable  $^{244}\text{Pu}$  is not an absolutely conclusive argument.

The second method that was used to

test whether a supernova was responsible for the iridium anomaly involved a measurement of the isotopic ratio of iridium in the boundary material. Iridium has two stable isotopes, 191 and 193, which would be expected to occur in about the same relative abundances, 37.3 to 62.7 percent, in all solar system mate-

rial because of mixing the protosolar gas cloud. However, different supernovas should produce iridium with different isotopic ratios because of differences in the contributions of the *r* and *s* processes occasioned by variations in neutron fluxes, reaction times, and so on, from one supernova to the next. According to this generally accepted picture, solar system iridium is a mixture of that element produced by all the supernovas that ejected material into the gaseous nebula that eventually condensed to form the sun and its planets. A particular supernova would produce Ir with an isotopic ratio that might differ from that of solar system material by as much as a factor of 2 (52).

We therefore compared the isotopic ratio of Ir from the C-T boundary clay with that of ordinary Ir, using NAA. This is a new technique (23), which we developed because of the extreme difficulty of determining Ir isotope ratios by mass spectrometry. In our earlier analytical work we used only the 74-day  $^{192}\text{Ir}$ , made from  $^{191}\text{Ir}$  by neutron capture. But in this new work we also measured the 18-hour  $^{194}\text{Ir}$  made from the heavier Ir isotope, and extensive chemical separations before and after the neutron irradiations were necessary. Figure 13 contrasts a typical gamma-ray spectrum of the kind used in the isotopic ratio measurement with one used in an Ir abundance determination. This comparison demonstrates the need for chemical purification of the iridium fraction as well as the lack of major interfering radiations.

The final result is that the isotopic ratio of the boundary Ir differs by only  $0.03 \pm 0.65$  percent (mean + 1 standard deviation) from that of the standard. From this, we conclude that the  $^{191}\text{Ir}/^{193}\text{Ir}$  ratio in the boundary layer and the standard do not differ significantly by more than 1.5 percent. Therefore the anomalous Ir is very likely of solar system origin, and did not come from a supernova or other source outside the solar system (53)—for example, during passage of the earth through the galactic arms. [In a very recent paper, Napier and Clube suggest that catastrophic events could arise from the latter (54).]

### The Asteroid Impact Hypothesis

After obtaining negative results in our tests of the supernova hypothesis, we were left with the question of what extraterrestrial source within the solar system could supply the observed iridium and also cause the extinctions. We consid-

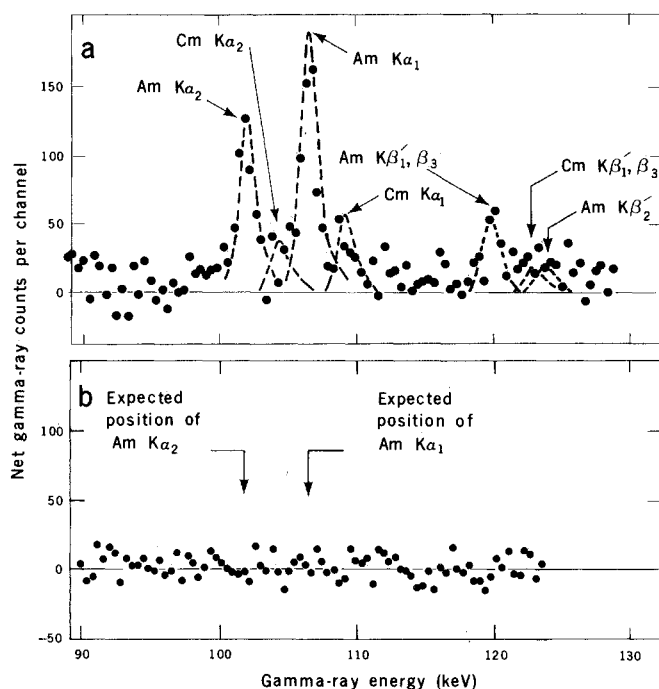


Fig. 12. Gamma-ray spectra of Pu fractions from acid-insoluble residues of irradiated boundary layer clay samples from Gubbio. (a) Sample had been spiked with  $^{244}\text{Pu}$  and  $^{238}\text{Pu}$  containing relatively small amounts of  $^{239}\text{Pu}$ ,  $^{240}\text{Pu}$ , and  $^{242}\text{Pu}$ . Dashed lines show expected energies and abundances of  $^{245}\text{Pu}$  and equilibrated daughter radiations normalized to the 327.2-keV gamma ray of  $^{245}\text{Pu}$  (not shown). (b) Sample had been spiked with  $^{238}\text{Pu}$  containing relatively small amounts of  $^{239}\text{Pu}$ ,  $^{240}\text{Pu}$ , and  $^{242}\text{Pu}$ . No  $^{244}\text{Pu}$  was detected.

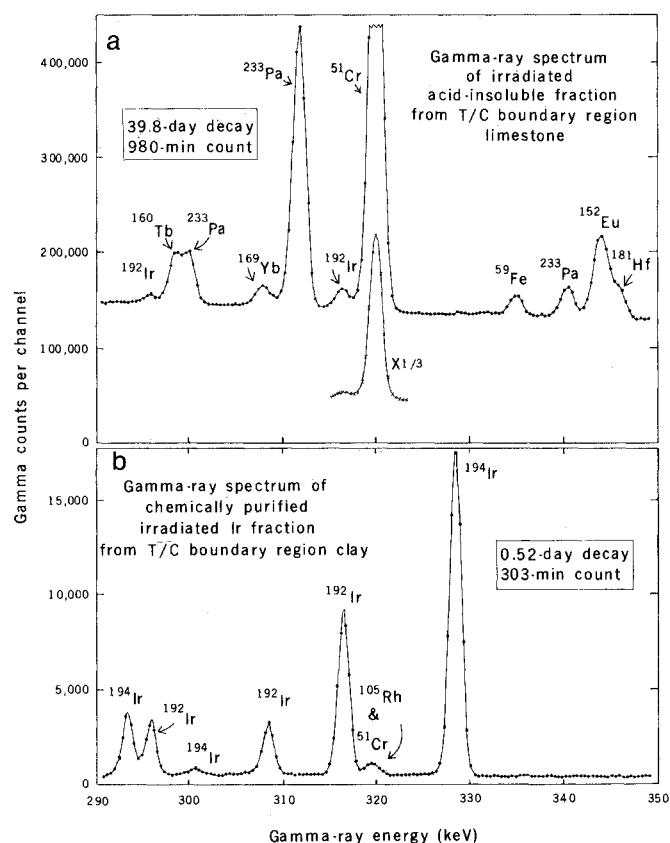


Fig. 13. (a) Gamma-ray spectrum of irradiated acid-insoluble residue from boundary layer clay at Gubbio without chemistry before or after irradiation. (b) Same as above with chemistry before and after irradiation used in isotopic ratio determinations. Counting periods, decay periods, and chemical yields are different for the two spectra.

ered and rejected a number of hypotheses (23); finally, we found that an extension of the meteorite impact hypothesis (55, 56) provided a scenario that explains most or all of the biological and physical evidence. In brief, our hypothesis suggests that an asteroid struck the earth, formed an impact crater, and some of the dust-sized material ejected from the crater reached the stratosphere and was spread around the globe. This dust effectively prevented sunlight from reaching the surface for a period of several years, until the dust settled to earth. Loss of sunlight suppressed photosynthesis, and as a result most food chains collapsed and the extinctions resulted. Several lines of evidence support this hypothesis, as discussed in the next few sections. The size of the impacting object can be calculated from four independent sets of observations, with good agreement among the four different diameter estimates.

#### Earth-Crossing Asteroids and Earth Craters

Two quite different data bases show that for the last billion years the earth has been bombarded by a nearly constant flux of asteroids that cross the earth's orbit. One data base comes from astronomical observations of such asteroids and a tabulation of their orbital parameters and their distribution of diameters (57). Öpik (58) computed that the mean time to collision with the earth for a given earth-crossing asteroid is about 200 million years. To a first approximation, the number of these objects with diameters greater than  $d$  drops roughly as the inverse square of  $d$ . E. M. Shoemaker [cited in (59, 60)] and Wetherill (60) independently estimated that there are at present about 700 earth-crossing asteroids with diameters greater than 1 km (Apollo objects), so there should be about seven with diameters greater than 10 km. This assumes that the power law with exponent  $-2$  extends from the accessible 1-km-diameter range into the 10-km-diameter range. If one accepts the numbers given above, the mean time to collision for an earth-crossing asteroid with a diameter of 10 km or more would be 200 million years divided by 7, or  $\sim 30$  million years. In a more sophisticated calculation, Shoemaker (61) estimates that a mean collision time of 100 million years is consistent with a diameter of 10 km, which is the value we will adopt. A discussion of cratering data, which leads to similar estimates, is given

in Grieve and Robertson's review article (62) on the size and age distribution of large impact craters on the earth. Rather than present our lengthy justification (23) for the estimates based on the cratering data, we will simply report the evaluation of Grieve (63), who wrote: "I can find nothing in your data that is at odds with your premise." Grieve also estimates that the diameter of the crater formed by the impact of a 10-km asteroid would be about 200 km (63). This section of our article has thus been greatly condensed now that we have heard from experienced students of the two data bases involved.

#### Krakatoa

The largest well-studied terrestrial explosion in historical times was that of the island volcano, Krakatoa, in the Sunda Strait, between Java and Sumatra (64). Since this event provides the best available data on injection of dust into the stratosphere, we give here a brief summary of relevant information.

On 26 and 27 August 1883, Krakatoa underwent volcanic eruptions that shot an estimated  $18 \text{ km}^3$  of material into the atmosphere, of which about  $4 \text{ km}^3$  ended up in the stratosphere, where it stayed for 2 to 2.5 years. Dust from the explosion circled the globe, quickly giving rise to brilliant sunsets seen worldwide. Recent measurements of the  $^{14}\text{C}$  injected into the atmosphere by nuclear bomb tests confirm the rapid mixing (about 1 year) between hemispheres (65). If we take the estimated dust mass in the stratosphere ( $4 \text{ km}^3$  times the assumed low density of  $2 \text{ g/cm}^3$ ) and spread it uniformly over the globe, it amounts to  $1.6 \times 10^{-3} \text{ g/cm}^2$ . This layer did not absorb much of the incident radiation on a "straight-through" basis. However, if it were increased by a factor of about  $10^3$  (a rough prediction of our theory), it is most probable that the sunlight would be attenuated to a high degree.

Since the time for the colored sunsets to disappear after Krakatoa is frequently given as 2 to 2.5 years, we have assumed that the asteroid impact material in the stratosphere settled in a few years. Thus, 65 million years ago, day could have been turned into night for a period of several years, after which time the atmosphere would return relatively quickly to its normal transparent state.

What happened during the Krakatoa explosions can be expected to happen to a much greater extent during the impact of a large asteroid. An interesting dif-

ference is that extreme atmospheric turbulence would follow the impact. The asteroid would enter the atmosphere at roughly 25 km/sec and would "punch a hole" in the atmosphere about 10 km across. The kinetic energy of the asteroid is approximately equivalent to that of  $10^8$  megatons of TNT.

#### Size of the Impacting Object

If we are correct in our hypothesis that the C-T extinctions were due to the impact of an earth-crossing asteroid, there are four independent ways to calculate the size of the object. The four ways and the results obtained are outlined below.

1) The postulated size of the incoming asteroid was first computed from the iridium measurements in the Italian sections, the tabulated Ir abundances (66) in type I carbonaceous chondrites (CI), which are considered to be typical solar system material, and the fraction of erupted material estimated to end up in the stratosphere. If we neglect the latter fraction for the moment, the asteroid mass is given by  $M = sA/f$ , where  $s$  is the surface density of Ir (measured at Gubbio to be  $8 \times 10^{-9} \text{ g/cm}^2$ ),  $A$  is the surface area of the earth, and  $f$  is the Ir mass fractional abundance in CI meteorites ( $0.5 \times 10^{-6}$ ). This preliminary value of the asteroid mass,  $7.4 \times 10^{16} \text{ g}$ , is then divided by the estimated fraction staying in the stratosphere, 0.22, to give  $M = 3.4 \times 10^{17} \text{ g}$ . The "Krakatoa fraction," 0.22, is used simply because it is the only relevant number available. It could differ seriously from the correct value, however, as the two explosions are of quite different character. At a density of  $2.2 \text{ g/cm}^3$  (67), the diameter of the asteroid would be 6.6 km.

2) The second estimate comes from data on earth-crossing asteroids and the craters they have made on the earth's surface. In a sense, the second estimate comes from two quite different data bases—one from geology and the other from astronomy. Calculations of the asteroid diameter can be made from both data bases, but they will not really be independent since the two data bases are known to be consistent with each other. As shown in an earlier section, the most believable calculation of the mean time between collisions of the earth and asteroids equal to or larger than 10 km in diameter is about 100 million years. The smaller the diameter the more frequent are the collisions, so our desire to fit not only the C-T extinction, but earlier ones as well, sets the mean time between ex-



tinctions at about 100 million years and the diameter at about 10 km.

3) The third method of estimating the size of the asteroid comes from the possibility that the 1-cm boundary layer at Gubbio and Copenhagen is composed of material that fell out of the stratosphere, and is not related to the clay that is mixed in with the limestone above and below it. This is quite a surprising prediction of the hypothesis, since the most obvious explanation for the origin of the clay is that it had the same source as the clay impurity in the rest of the Cretaceous and Tertiary limestone, and that it is nearly free of primary  $\text{CaCO}_3$  because the extinction temporarily destroyed the calcite-producing plankton for about 5000 years. But as discussed earlier, the material in the boundary layer is of a different character from the clay above and below it, whereas the latter two clays are very similar. To estimate the diameter of the asteroid, one can use the surface density of the boundary layer (about  $2.5 \text{ g/cm}^2$ ), together with an estimate of the fraction of that material which is of asteroidal origin. The asteroid diameter is then calculated to be 7.5 km. The numbers used in this calculation are the following: clay fraction in the boundary layer, 0.5; density of the asteroid,  $2.2 \text{ g/cm}^3$ ; mass of crustal material thrown up per unit mass of asteroid,  $\sim 60$  (63); fraction of excavated material delivered to the stratosphere, 0.22 (from the Krakatoa measurements). If one uses different numbers, the diameter changes only by the cube root of the ratio of input values.

The first and the third methods are independent, even though they both depend on measurements made on the boundary material. This can best be appreciated by noting that if the Ir abundance were about the same in the earth's crust as it is in meteorites, the iridium anomaly seen in Fig. 5 would not exist. Therefore, method 1 would not exist either. The fact that method 3 could still be used is the indicator of the relative independence of the two methods.

4) The fourth method is not yet able to set close limits on the mass of the incoming asteroid, but it leads to consistent results. This method derives from the need to make the sky much more opaque than it was in the years following the Krakatoa explosion. If it is assumed that the Krakatoa dust cloud attenuated the vertically incident sunlight by about 3 percent, then an explosion involving 33 times as much material would reduce the light intensity to  $1/e$ . The stratospheric mass due to an explosion of the magnitude calculated in the three earlier meth-

ods—about 1000 times that of Krakatoa—would then be expected to reduce the sunlight to  $\exp(-30) = 10^{-13}$ . This is, of course, much more light attenuation than is needed to stop photosynthesis. But the model used in this simplistic calculation assumes that the dust is a perfect absorber of the incident light. A reasonable albedo coupled with a slight reduction in the mass of dust can raise the light intensity under the assumed "optical depth" to  $10^{-7}$  of normal sunlight, corresponding to 10 percent of full moonlight.

Although it is impossible to make an accurate estimate of the asteroid's size from the Krakatoa extrapolation, it would have been necessary to abandon the hypothesis had a serious discrepancy been apparent. In the absence of good measurements of the solar constant in the 1880's, it can only be said that the fourth method leads to asteroid sizes that are consistent with the other three.

Until we understand the reasons for the factor of 10 difference in Ir content of the boundary clay between Denmark and Italy, we will be faced with different values for the asteroid diameter based on the first method. The "Danish diameter" is then  $6.6 \text{ km} \times 10^{1/3} = 14 \text{ km}$ . The second and third estimates are unchanged; the second does not involve measurements made on the boundary layer, and the third uses the thickness of the clay, which is only slightly greater in Denmark than in Italy. The fourth method is based on such an uncertain attenuation value, from Krakatoa, that it is not worth recalculating. We conclude that the data are consistent with an impacting asteroid with a diameter of about  $10 \pm 4 \text{ km}$ .

### Biological Effects

A temporary absence of sunlight would effectively shut off photosynthesis and thus attack food chains at their origins. In a general way the effects to be expected from such an event are what one sees in the paleontological record of the extinction.

The food chain in the open ocean is based on microscopic floating plants, such as the coccolith-producing algae, which show a nearly complete extinction. The animals at successively higher levels in this food chain were also very strongly affected, with nearly total extinction of the foraminifera and complete disappearance of the belemnites, ammonites, and marine reptiles.

A second food chain is based on land plants. Among these plants, existing individuals would die, or at least stop pro-

ducing new growth, during an interval of darkness, but after light returned they would regenerate from seeds, spores, and existing root systems. However, the large herbivorous and carnivorous animals that were directly or indirectly dependent on this vegetation would become extinct. Russell (2) states that "no terrestrial vertebrate heavier than about 25 kg is known to have survived the extinctions." Many smaller terrestrial vertebrates did survive, including the ancestral mammals, and they may have been able to do this by feeding on insects and decaying vegetation.

The situation among shallow marine bottom-dwelling invertebrates is less clear; some groups became extinct and others survived. A possible base for a temporary food chain in this environment is nutrients originating from decaying land plants and animals and brought by rivers to the shallow marine waters.

We will not go further into this matter, but we refer the reader to the proceedings of the 1976 Ottawa meeting on the C-T extinctions. This volume reproduces an extensive discussion among the participants of what would happen if the sunlight were temporarily "turned off" (5, pp. 144-149). Those involved in the discussion seemed to agree that many aspects of the extinction pattern could be explained by this mechanism, although a number of puzzles remained.

We must note, finally, an aspect of the biological record that does not appear to be in accord with the asteroid impact hypothesis or with any sudden, violent mechanism. Extinction of the foraminifera and nannoplankton occurs within reversed geomagnetic polarity zone Gubbio G— in the Gubbio section (30). Butler and co-workers (68, 69) have studied the nonmarine sequence of the San Juan Basin of New Mexico and have found a polarity sequence that appears to be correlated with the reversal sequence at Gubbio. In the San Juan Basin, the highest dinosaur fossils are found in the normal polarity zone (anomaly 29) that follows what is identified as the Gubbio G— zone. It would thus appear that the dinosaur and foram-nannoplankton extinctions were not synchronous. (Extinctions occurring in the same polarity zone in distant sections would not establish either synchronicity or diachroneity.) Three comments on the San Juan Basin work have been published (70) calling attention to the possibility of an unconformity at the boundary, in which case the correlation of the magnetic polarity zones could be in error and the extinctions might still be synchronous. Lindsay *et al.* (69) argue strongly against

a major hiatus, but admit that "the case is not completely closed." Russell (71) has noted stratigraphic evidence against a diachronous extinction in the continental and marine realm.

Resolution of the question of whether the extinctions could have been synchronous will depend on further paleomagnetic studies. In the meantime we can state that the asteroid impact hypothesis predicts that the apparently diachronous timing of the foram-nannofossil and dinosaur extinctions will eventually be shown to be incorrect.

### Problems in Boundary Clay Composition

One would expect from the simplest considerations of our hypothesis that the boundary layer resulted from crustal material (enriched in certain elements by the asteroidal matter) that was distributed worldwide in the stratosphere and then fell into the ocean. This material would be subjected to chemical and physical processes in the atmosphere and then in the ocean, which would alter the composition. The enhancements of metals having water-insoluble sulfides in the Danish C-T boundary compared to the Italian might be related to an anaerobic environment during deposition of the former and an aerobic one for the latter. Hydrogen sulfide can be produced by bacteria in oxygen-deficient waters, and this would precipitate those metals if they were available. This would not, however, explain the striking depletion of some trace elements in the Danish boundary or its very high Ir abundance. If chondritic Ir with an abundance of ~ 500 ppb were diluted 60-fold with crustal material, the Ir abundance should be ~ 8 ppb rather than the 65 ppb observed. Possible solutions to these difficulties may arise when better estimates of the extent of mixing of asteroidal and terrestrial material in the atmosphere are made, and when the boundary layer chemistry is studied at additional locations and a better understanding of the marine chemistry is achieved.

### Implications

Among the many implications of the asteroid impact hypothesis, if it is correct, two stand out prominently. First, if the C-T extinctions were caused by an impact event, the same could be true of the earlier major extinctions as well. There have been five such extinctions since the end of the Precambrian, 570 million years ago, which matches well

the probable interval of about 100 million years between collisions with 10-km-diameter objects. Discussions of these extinction events generally list the organisms affected according to taxonomic groupings; it would be more useful to have this information given in terms of interpreted ecological or food-chain groupings. It will also be important to carry out iridium analyses in complete stratigraphic sections across these other boundaries. However, E. Shoemaker (private communication) predicts that if some of the extinctions were caused by the collision of a "fresh" comet (mostly ice), the Ir anomaly would not be seen even though the extinction mechanism was via the same dust cloud of crustal material, so the absence of a higher Ir concentration at, for example, the Permian-Triassic boundary would not invalidate our hypothesis. According to Shoemaker, cometary collisions in this size range could be twice as frequent as asteroidal collisions.

Second, we would like to find the crater produced by the impacting object. Only three craters 100 km or more in diameter are known (62). Two of these (Sudbury and Vredefort) are of Precambrian age. For the other, Popigay Crater in Siberia, a stratigraphic age of Late Cretaceous to Quaternary and a potassium-argon date of 28.8 million years (no further details given) have been reported (72, 73). Thus, Popigay Crater is probably too young, and at 100-km-diameter probably also too small, to be the C-T impact site. There is about a 2/3 probability that the object fell in the ocean. Since the probable diameter of the object, 10 km, is twice the typical oceanic depth, a crater would be produced on the ocean bottom and pulverized rock could be ejected. However, in this event we are unlikely to find the crater, since bathymetric information is not sufficiently detailed and since a substantial portion of the pre-Tertiary ocean has been subducted.

### References and Notes

1. D. A. Russell, *Geol. Assoc. Can. Spec. Rep.* 13 (1975), p. 119.
2. —, in (5), p. 11.
3. M. B. Cita and I. Premoli Silva, *Riv. Ital. Paleontol. Stratigr. Mem.* 14 (1974), p. 193.
4. D. A. Russell, *Annu. Rev. Earth Planet. Sci.* 7, 163 (1979).
5. K-TEC group (P. Béland et al.), *Cretaceous-Tertiary Extinctions and Possible Terrestrial and Extraterrestrial Causes* (Proceedings of Workshop, National Museum of Natural Sciences, Ottawa, 16 and 17 Nov. 1976).
6. T. Birkelund and R. G. Bromley, Eds., *Cretaceous-Tertiary Boundary Events*, vol. 1, *The Maastrichtian and Danian of Denmark* (Symposium, University of Copenhagen, Copenhagen, 1979); W. K. Christiansen and T. Birkelund, Eds., *ibid.*, vol. 2, *Proceedings*.
7. H. Tappan, *Palaeogeogr. Palaeoclimatol. Palaeoecol.* 4, 187 (1968); T. R. Worsley, *Nature (London)* 230, 318 (1971); W. T. Holser, *ibid.* 267, 403 (1977); D. M. McLean, *Science* 200, 1060 (1978); *ibid.* 201, 401 (1978); S. Gartner and J. Keany, *Geology* 6, 708 (1978).
8. E. G. Kauffman, in (6), vol. 2, p. 29.
9. A. G. Fischer, in (6), vol. 2, p. 11; — and M. A. Arthur, *Soc. Econ. Paleontol. Mineral. Spec. Publ.* 25 (1977), p. 19.
10. J. F. Simpson, *Geol. Soc. Am. Bull.* 77, 197 (1966); J. D. Hays, *ibid.* 82, 2433 (1971); C. G. A. Harrison and J. M. Prospero, *Nature (London)* 250, 563 (1974).
11. O. H. Schindewolf, *Neues Jahrb. Geol. Palaeontol. Monatsh.* 1954, 451 (1954); *ibid.* 1958, 270 (1958); A. R. Leoblich, Jr., and H. Tappan, *Geol. Soc. Am. Bull.* 75, 367 (1964); V. I. Krasovskii and I. S. Shklovskii, *Dokl. Akad. Nauk SSSR* 116, 197 (1957); K. D. Terry and W. H. Tucker, *Science* 159, 421 (1968); H. Laster, *ibid.* 160, 1138 (1968); W. H. Tucker and K. D. Terry, *ibid.*, p. 1138; D. Russell and W. H. Tucker, *Nature (London)* 229, 553 (1971); M. A. Ruderman, *Science* 184, 1079 (1974); R. C. Whitten, J. Cuzzi, W. J. Borucki, J. H. Wolfe, *Nature (London)* 263, 398 (1976).
12. S. Gartner and J. P. McGuirk, *Science* 206, 1272 (1979).
13. A. Boersma and N. Schackleton, in (6), vol. 2, p. 50; B. Buchardt and N. O. Jorgensen, in (6), vol. 2, p. 54.
14. L. Christensen, S. Fregerslev, A. Simonsen, J. Thiede, *Bull. Geol. Soc. Den.* 22, 193 (1973).
15. N. O. Jorgensen, in (6), vol. 1, p. 33, vol. 2, p. 62; M. Renard, in (6), vol. 2, p. 70.
16. H. P. Luterbacher and I. Premoli Silva, *Riv. Ital. Paleontol. Stratigr.* 70, 67 (1964).
17. H. Pettersson and H. Rotschi, *Geochim. Cosmochim. Acta* 2, 81 (1952).
18. V. M. Goldschmidt, *Geochemistry* (Oxford Univ. Press, New York, 1954).
19. J. L. Barker, Jr., and E. Anders, *Geochim. Cosmochim. Acta* 32, 627 (1968).
20. R. Ganapathy, D. E. Brownlee, P. W. Hodge, *Science* 201, 1119 (1978).
21. A. M. Sarna-Wojcicki, H. R. Bowman, D. Marchand, E. Helley, private communication.
22. J. H. Crockett and H. Y. Kuo, *Geochim. Cosmochim. Acta* 43, 831 (1979).
23. These are briefly discussed in L. W. Alvarez, W. Alvarez, F. Asaro, H. V. Michel, *Univ. Calif. Lawrence Berkeley Lab. Rep. LBL-9666* (1979).
24. A description of the NAA techniques is given in Alvarez et al. (23), appendix II; I. Perlman and F. Asaro, in *Science and Archaeology*, R. H. Brill, Ed. (MIT Press, Cambridge, Mass., 1971), p. 182.
25. These limestones belong to the Umbrian sequence, of Jurassic to Miocene age, which has been described in V. Bortolotti, P. Passerini, M. Saggi, G. Sestini, *Sediment. Geol.* 4, 341 (1970); A. Jacobacci, E. Centamore, M. Chiochini, N. Malferrari, G. Martelli, A. Micarelli, *Note Esplicative Carta Geologica d'Italia (1:50,000), Foglio 190: "Cagli"* (Rome, 1974).
26. H. P. Luterbacher and I. Premoli Silva, *Riv. Ital. Paleontol. Stratigr.* 68, 253 (1962); I. Premoli Silva, L. Paggi, S. Monechi, *Mem. Soc. Geol. Ital.* 15, 21 (1976).
27. S. Monechi, in (6), vol. 2, p. 164.
28. D. V. Kent, *Geology* 5, 769 (1977); M. A. Arthur, thesis, Princeton University (1979).
29. O. Renz, *Eclogae Geol. Helv.* 29, 1 (1936); *Serv. Geol. Ital. Mem. Descr. Carta Geol. Ital.* 29, 1 (1936).
30. M. A. Arthur and A. G. Fischer, *Geol. Soc. Am. Bull.* 88, 367 (1977); I. Premoli Silva, *ibid.*, p. 371; W. Lowrie and W. Alvarez, *ibid.*, p. 374; W. M. Roggenthen and G. Napoleone, *ibid.*, p. 378; W. Alvarez, M. A. Arthur, A. G. Fischer, W. Lowrie, G. Napoleone, I. Premoli Silva, W. M. Roggenthen, *ibid.*, p. 383; W. Lowrie and W. Alvarez, *Geophys. J. R. Astron. Soc.* 51, 561 (1977); W. Alvarez and W. Lowrie, *ibid.* 55, 1 (1978).
31. Locations of the sections studied are: (i) Bottaccione Gorge at Gubbio: 43°21.9'N, 12°35.0'E (0°7.9' east of Rome); (ii) Contessa Valley, 3 km northwest of Gubbio: 43°22.6'N, 12°33.7'E (0°6.6' east of Rome); (iii) Petriccio suspension bridge, 2.3 km west-southwest of Acqualagna: 43°36.7'N, 12°38.7'E (0°11.6' east of Rome); (iv) Acqualagna, road cut 0.8 km southeast of town: 43°36.7'N, 12°40.8'E (0°13.7' east of Rome); and (v) Gorgo a Cerbara: 43°36.1'N, 12°33.6'E (0°6.5' east of Rome). We thank E. Sannipoli, W. S. Leith, and S. Marshak for help in sampling these sections.
32. J. H. Crockett, J. D. McDougall, R. C. Harris, *Geochim. Cosmochim. Acta* 37, 2547 (1973).
33. Location: 55°16.7'N, 12°26.5'E. We thank I. Bank and S. Gregersen for taking W.A. to this locality.
34. A. Rosenkrantz and H. W. Rasmussen, *Guide to Excursions A42 and C37* (21st International



- Geological Congress, Copenhagen, 1960), part 1, pp. 1-17.
35. F. Surlyk, in (6), vol. 1, p. 164.
  36. C. Heinberg, in (6), vol. 1, p. 58.
  37. H. W. Rasmussen, in (6), vol. 1, p. 65; P. Graven, in (6), vol. 1, p. 72; U. Asgaard, in (6), vol. 1, p. 74.
  38. E. Hakansson and E. Thomsen, in (6), vol. 1, p. 78.
  39. S. Floris, in (6), vol. 1, p. 92.
  40. I. Bang, in (6), vol. 1, p. 108.
  41. K. Perch-Nielsen, in (6), vol. 1, p. 115.
  42. Soft x-ray fluorescence measurements for major element determinations were made by S. Flexser and M. Sturz of Lawrence Berkeley Laboratory.
  43. Hard x-ray fluorescence measurements for trace element determinations were made by R. D. Giauque of Lawrence Berkeley Laboratory.
  44. F. G. Walton Smith, Ed. *CRC Handbook of Marine Science* (CRC Press, Cleveland, 1974), vol. 1, p. 11.
  45. H. A. Wollenberg et al., *Univ. Calif. Lawrence Berkeley Lab. Rep. LBL-7092*, revised 1980.
  46. *Encyclopaedia Britannica* (Benton, Chicago, ed. 15, 1974), vol. 6, p. 702.
  47. K. K. Turekian, *Oceans* (Prentice-Hall, Englewood Cliffs, N.J., 1976), p. 122.
  48. J. H. Crocket, *Can. Mineral.* 17, 391 (1979); J. R. Ross and R. Keays, *ibid.*, p. 417.
  49. I. S. Shklovsky, *Supernovae* (Wiley, New York, 1968), p. 377.
  50. D. D. Clayton, *Principles of Stellar Evolution and Nucleosynthesis* (McGraw-Hill, New York, 1968), pp. 546-606.
  51. D. N. Schramm, *Annu. Rev. Astron. Astrophys.* 12, 389 (1974).
  52. C. F. McKee, personal communication.
  53. These observations were reported at the American Geophysical Union meeting in May 1979 and at the Geological Society of America meeting in November 1979 [W. Alvarez, L. W. Alvarez, F. Asaro, H. V. Michel, *Eos* 60, 734 (1979); *Geol. Soc. Am. Abstr. Programs* 11, 350 (1979)].
  54. W. M. Napier and S. V. M. Clube, *Nature (London)* 282, 455 (1979).
  55. H. C. Urey, *ibid.* 242, 32 (1973).
  56. E. J. Öpik, *Ir. Astron. J.* 5 (No. 1), 34 (1958).
  57. E. M. Shoemaker, J. G. Williams, E. F. Helin, R. F. Wolfe, in *Asteroids*, T. Gehrels, Ed. (Univ. of Arizona Press, Tucson, 1979), pp. 253-282.
  58. E. J. Öpik, *Adv. Astron. Astrophys.* 2, 220 (1963); *ibid.* 4, 302 (1964); *ibid.* 8, 108 (1971). These review articles give references to Öpik's extensive bibliography on meteorites, Apollo objects, and asteroids.
  59. C. R. Chapman, J. G. Williams, W. K. Hartmann, *Annu. Rev. Astron. Astrophys.* 16, 33 (1978).
  60. G. W. Wetherill, *Sci. Am.* 240 (No. 3), 54 (1979).
  61. E. M. Shoemaker, personal communication.
  62. R. A. F. Grieve and P. B. Robertson, *Icarus* 38, 212 (1979).
  63. R. A. F. Grieve, personal communication.
  64. G. J. Symons, Ed., *The Eruption of Krakatoa and Subsequent Phenomena* (Report of the Krakatoa Committee of the Royal Society, Harrison, London, 1888).
  65. I. U. Olson and I. Karlen, *Am. J. Sci. Radiocarbon Suppl.* 7 (1965), p. 331; T. A. Rafter and B. J. O'Brien, *Proc. 8th Int. Conf. Radiocarbon Dating* 1, 241 (1972).
  66. U. Krähenbühl, *Geochim. Cosmochim. Acta* 37, 1353 (1973).
  67. B. Mason, *Space Sci. Rev.* 1, 621 (1962-1963).
  68. R. F. Butler, E. H. Lindsay, L. L. Jacobs, N. M. Johnson, *Nature (London)* 267, 318 (1977); E. H. Lindsay, L. L. Jacobs, R. F. Butler, *Geology* 6, 425 (1978).
  69. E. H. Lindsay, R. F. Butler, N. M. Johnson, in preparation.
  70. W. Alvarez and D. W. Vann, *Geology* 7, 66 (1979); J. E. Fassett, *ibid.*, p. 69; S. G. Lucas and J. K. Rigby, Jr., *ibid.*, p. 323.
  71. D. A. Russell, *Episodes* 1979 No. 4 (1979), p. 21.
  72. V. L. Masaytis, M. V. Mikhaylov, T. V. Selivanovskaya, *Sov. Geol. No. 6* (1971), pp. 143-147; translated in *Geol. Rev.* 14, 327 (1972).
  73. V. L. Masaytis, *Sov. Geol. No. 11* (1975), pp. 52-64; translated in *Int. Geol. Rev.* 18, 1249 (1976).
  74. It will be obvious to anyone reading this article that we have benefited enormously from conversations and correspondence with many friends and colleagues throughout the scientific community. We would particularly like to acknowledge the help we have received from E. Anders, J. R. Arnold, M. A. Arthur, A. Buffington, I. S. E. Carmichael, G. Curtis, P. Eberhard, S. Gartner, R. L. Garwin, R. A. F. Grieve, E. K. Hyde, W. Lowrie, C. McKee, M. C. Michel (who was responsible for the mass spectrometric measurements), J. Neil, B. M. Oliver, C. Orth, B. Pardo, I. Perlman, D. A. Russell, A. M. Sessler, and E. Shoemaker. One of us (W.A.) thanks the National Science Foundation for support, the other three authors thank the Department of Energy for support, and one of us (L.W.A.) thanks the National Aeronautics and Space Administration for support. The x-ray fluorescence measurements of trace elements Fe and Ti by R. D. Giauque and of major elements by S. Flexser and M. Sturz were most appreciated. We appreciate the assistance of D. Jackson and C. Nguyen in the sample preparation procedures. We are grateful to T. Lim and the staff of the Berkeley Research Reactor for many neutron irradiations used in this work. We also appreciate the efforts of G. Pefley and the staff of the Livermore Pool Type Reactor for the irradiations used for the Ir isotopic ratio measurements.

## No-Tillage Agriculture

Ronald E. Phillips, Robert L. Blevins, Grant W. Thomas  
Wilbur W. Frye, Shirley H. Phillips

For over 100 years, agriculture has relied upon the moldboard plow and disk harrow to prepare soil to produce food. Without the moldboard plow and disk it would not have been possible to control weeds and to obtain the yields necessary to provide favorable economic returns from agriculture. Weeds are strong competitors with food crops for water and plant nutrients, and it was not until plant growth regulators were introduced in the late 1940's that attention was turned to no-tillage agriculture. From plant growth regulators selective herbicides were developed, and these increased the feasibility

of growing many different crops without tilling the soil (1-3).

In this article, we define conventional tillage as moldboard plowing followed by disking one or more times. By this method one obtains a loose, friable seedbed in the surface 10 centimeters of soil. We define the no-tillage system (4) as one in which the crop is planted either entirely without tillage or with just sufficient tillage to allow placement and coverage of the seed with soil to allow it to germinate and emerge. Usually no further cultivation is done before harvesting. Weeds and other competing vegetation are controlled by chemical herbicides. Soil amendments, such as lime and fertilizer, are applied to the soil surface.

In pasture management, chemicals are used as a substitute for tillage, herbicides being used to restrict growth and com-

petition of undesirable plants during the establishment of the newly seeded crop or to suppress growth of grasses and allow establishment of legumes. Row crop production with the no-tillage system is almost always carried out by planting the crop into soil covered by a chemically killed grass sod or with dead plant residues of a previous crop. For example, in continuous no-tillage corn (*Zea mays*) production, the soil surface at the time of planting is covered with corn stalk residues of the previous corn crop. In double-cropped soybeans, the soil at the time of planting is covered with residues of a recently harvested small-grain crop such as barley or wheat.

The land area used for row crops and forage crops grown by the no-tillage system has increased rapidly during the past 15 years. In 1974, the U.S. Department of Agriculture (5) estimated that the amount of cropland in the United States under no-tillage cultivation was 2.23 million hectares, and that 62 million hectares or 45 percent of the total U.S. cropland (6) will be under the no-tillage system by 2000. An estimated 65 percent of the seven major annual crops (corn, soybeans, sorghum, wheat, oats, barley, and rye) will be grown by the no-tillage system by the year 2000 and 78 percent by the year 2010 (5). In Kentucky there were 44,000, 160,400, and 220,000 ha of no-tillage corn and soybeans grown in 1969, 1972, and 1978, respectively.

R. E. Phillips and G. W. Thomas are professors and R. L. Blevins and W. W. Frye are associate professors in the Department of Agronomy, College of Agriculture, University of Kentucky, Lexington 40546. S. H. Phillips is assistant director of the Cooperative Extension Service for Agriculture, Lexington 40546.